



Fractional Order PID Control for Solar PV- Wind and Battery Storage Systems using Three Phase Inverter

¹.Bobde Tushar Tejrao , ²Prof. K. Chandra Obula Reddy , ³Prof. Uddhav G.Takle,
¹Mtech Electrical Power System, ²Assistant Professor,HOD ³ Prof, Department of Electrical Engineering
¹M.S.S College of Engineering, Jalna, India

Abstract— in this paper, a novel configuration of a Three Phase inverter that can integrate solar photovoltaic (PV)- Wind with battery storage in a grid-connected system is proposed. The vigor of the proposed topology lies in a novel, elongated unbalance three-level vector modulation technique that can engender the correct ac voltage under unbalanced dc voltage conditions. This paper presents the Fractional order PID design philosophy of the proposed configuration and the theoretical framework of the proposed modulation technique. An incipient fraction order PID controller for the proposed system is additionally presented in order to control the puissance distribution between the solar PV, battery, and grid, which simultaneously provides maximum power point tracking (MPPT) operation for the solar PV. The efficacy of the proposed methodology is investigated by the simulation of several scenarios, including battery charging and discharging with different calibers of solar irradiation. The proposed methodology and topology is tested on MATLAB/SIMULINK Environment.

Index Terms—Battery storage, solar photovoltaic (PV), space vector modulation (SVM), three-level inverter.

I. Introduction

DUE to the world energy crisis and environmental quandaries caused by conventional power generation, renewable energy sources such as photovoltaic (PV) and wind generation systems are becoming more promising alternatives to supersede conventional generation units for electricity generation [1], [2]. Advanced power electronic systems are needed to utilize and develop renewable energy sources. In solar PV or wind energy applications, utilizing maximum power from the source is one of the most consequential functions of the potency electronic systems[3]–

[5]. In three-phase applications, two types of potency electronic configurations are commonly used to transfer power from the renewable energy resource to the grid:

Single-stage and double-stage conversion. In the Double-stage conversion for a PV system, the first stage is customarily a dc/dc converter and second stage is a dc/ac inverter. The function of the dc/dc converter is to facilitate the maximum power point tracking (MPPT) of the PV array and to engender the congruous dc voltage for the dc/ac inverter. The function of the inverter is to engender three-phase sinusoidal voltages or currents to transfer the potency to the grid in a grid-connected solar PV system or to the load in a stand-alone system [3]–[5]. In the single-stage connection, only one converter is needed to consummate the double-stage functions, and hence the system will have a lower cost and higher efficiency, however, a more intricate control method will be required. The current norm of the industry for high power applications is a three-phase, singlestagePV energy systems by utilizing a voltage-source converter(VSC) for power conversion [4]. One of the major concerns of solar and wind energy systems is their capricious and fluctuating nature. Grid-connected renewable energy systems accompanied by battery energy storage can surmount this concern. This withal can increment the flexibility of puissance system control and raise the overall availability of the system [2]. Conventionally, a converter is required to control the charging and discharging of the battery storage system and another converter is required for dc/ac power conversion; thus, a three-phasePV system connected to battery storage will require two converters. This paper is concerned with the design and study of a grid-connected three-phase solar PV system integrated with battery storage utilizing only one three-level converter having the capability of MPPT and ac-side current control, and withal the ability of controlling

the battery charging and discharging. This will result in lower cost, better efficiency and incremented flexibility of puissance flow control. The remnant of the paper is organized as follows. Section II describes the structure of a three-level inverter and associated capacitor voltages. Section III presents the proposed topology to integrate solar PV and battery storage and its associated control. Section IV describes the Fractional Order PID Controller Section V describes the simulation and validation of the proposed topology and associated control system. Section VI concludes the paper.

II. STRUCTURE OF A Three PHASE INVERTER

IV. Fractional Order PID Controller

A PID controller is a generic control loop feedback mechanism widely used in industrial control systems. The PID controller attempts to correct the error between a measured process variable and a desired set point by calculating and then outputting a corrective action that can adjust the process accordingly. An integer order PID controller has the following transfer function:

$$G_c(s) = K_p + K_i s^{-1} + K_d s$$

The PID controller calculation (algorithm) involves three separate parameters; the Proportional (K_p), the Integral (i K) and Derivative (d K) time-constants. The Proportional gain determines the reaction to the current error, the Integral determines the reaction based on the sum of recent errors and the derivative determines the reaction to the rate at which the error has been changing. The weighted sum of these three actions is used to adjust the process via a control element such as the position of a control valve or the power supply of a heating element. The block diagram of a generic closed loop control system with the PID controller is illustrated in Figure 5.

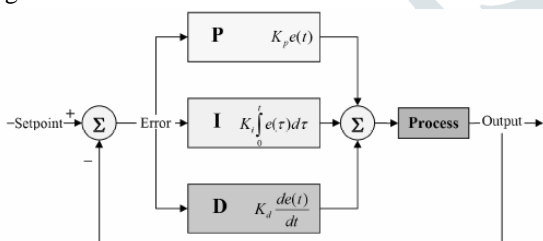


Figure 7. A generic closed-loop process-control system with PID controller

The real objects or processes that we want to control are generally fractional (for example, the voltage-current relation of a semi-infinite lossy RC line). However, for many of them the fractionality is very low. In general, the integer-order approximation of the fractional systems can cause significant differences between mathematical model and real system. The main reason for using integer-order models was the absence of solution methods for fractional-order differential equations. PID controllers belong to dominating industrial controllers and therefore are objects of steady effort for improvements of their quality and robustness. One of the possibilities to improve PID controllers is to use fractional-order controllers with non-integer derivation and

integration parts. Following the works of Podlubny [6] we may go for a generalization of the PID-controller, which can be called the PIλDμ-controller because of involving an integrator of order and a differentiator of order μ. The continuous transfer function of such a controller has the form:

$$G_c(s) = K_p + T_i s^{-\lambda} + T_d s^{\mu}, (\lambda, \mu > 0)$$

All these classical types of PID-controllers are the special cases of the fractional PIIDμ-controller. As depicted in Figure 2, the fractional order PID controller generalizes the integer order PID controller and expands it from point to plane. This expansion adds more flexibility to controller design and we can control our real world processes more accurately.

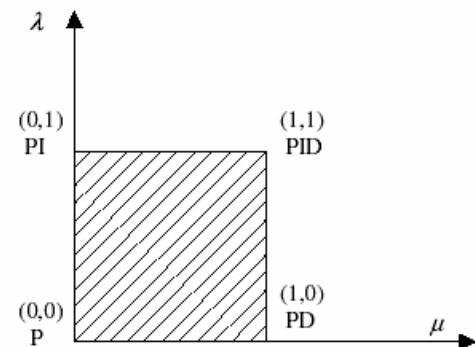


Figure 8. Generalization of the FOPID Controller: From point to plane

V. SIMULATION AND VALIDATION OF THE PROPOSED TOPOLOGY AND CONTROL SYSTEM

Simulations have been carried out using MATLAB/Simulink to verify the effectiveness of the proposed topology and control system. An LCL filter is used to connect the inverter to the grid. Fig. 8 shows the block diagram of the simulated system.

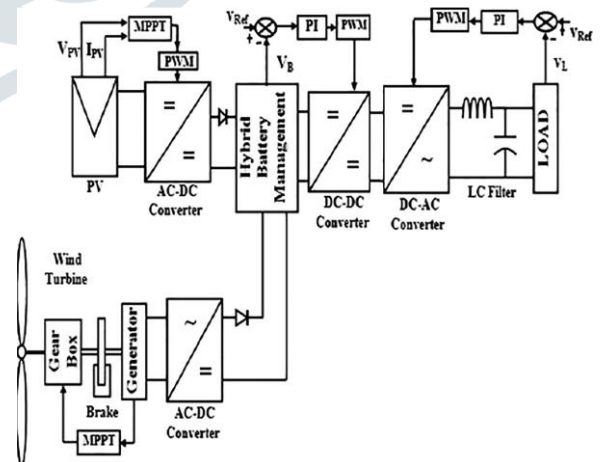
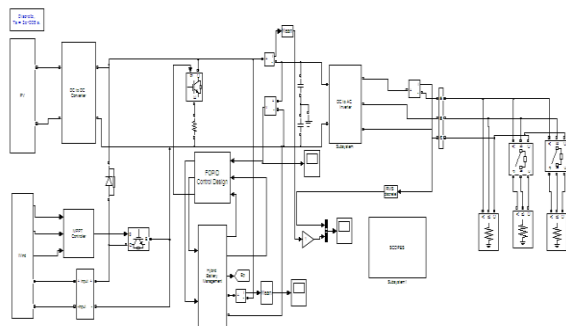
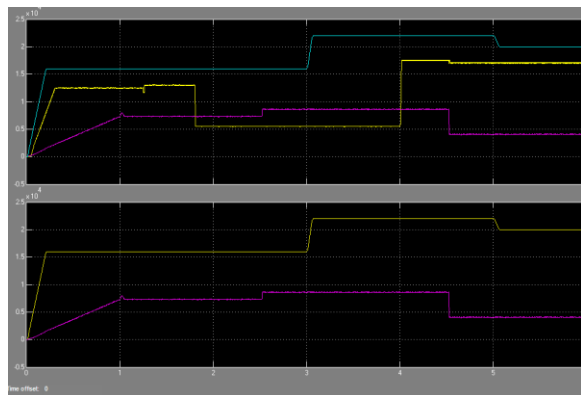


Fig. 8. Block diagram of the simulated system.



Simulation of the proposed system



Simulation results

TABLE I
PARAMETERS OF THE SIMULATED SYSTEM

V_{BAT}	V_s (line)	L_{BAT}	C_1, C_2	L_f	L_g
60 V	50 V	5 mH	1000 μ F	500 μ H	900 μ H
r_f	C_f	K_p	K_i	G_1	G_2
3 Ω	14 μ F	2.9	1700	1	200

Three, series-connected PV modules are used in the simulation. The mathematical model of each of the PV units is given in (21) [21] and used in the simulation where ISC is the short circuit current of the PV. In the simulation, it is assumed that ISC will change with different irradiances. With a solar irradiation of 1000 W/m², ISC is equal to 6.04 A and the open circuit voltage of the PV panels will be equal to $V_{oc} = 44V$. The main parameters of the simulated system are given in Table I. As discussed in Section III-B, G_2 must be much more than G_1 in order to achieve the MPPT condition and to have the flexibility to charge and discharge of the battery. Based on our experiments, any value more than 100 is suitable for this ratio. On the other hand, because the ratio of G_2 / G_1 will only affect the short-vector selection, increasing this ratio will not affect other results. This value has been selected to be 200 to have good control on V_{dc} , as shown in Table I. The role of L_{BAT} is to smooth the battery current, especially in the transient condition. A wide range of

values are acceptable for the inductor value, however, decreasing its value will increase the current overshoot of the battery. Also, its value is dependent of its adjacent capacitor value and its transient voltages. Due to the practical considerations (such as size and cost), the value of L_{BAT} is preferred to be low and has been chosen to be 5 mH based on our simulation studies. The values of K_p and K_i are selected by modeling the system in the dq -frame. The current control loop can be converted to a simple system after using the decoupling technique shown in Fig 7. The details of this method can be found in [22]. For theoretical purposes, two different scenarios have been simulated to investigate the effectiveness of the proposed topology and the control algorithm using a step change in the reference inputs under the following conditions:

- 1) The effect of a step change in the requested active underactive power to be transferred to the grid when the solar irradiance is assumed to be constant.
- 2) The effect of a step change of the solar irradiation when the requested active and reactive power to be transmitted to the grid is assumed to be constant. In a practical system, a slope controlled change in the reference input is usually used rather than a step change to reduce the risk of mathematical internal calculation errors when working with a limited precision microprocessor system and also to prevent the protection system activation. Furthermore, in practical situations, the inputs of the systems normally do not change instantaneously as a step change, such as the sun irradiation. With this practical application in mind, the proposed system is simulated using a slope controlled change in the requested active power to be transferred to the grid when the solar irradiance is assumed to be constant. To validate this, a laboratory test is carried out using the same scenario and the experimental results given in Section V can be compared with the results from this simulation.

A. First Theoretical Scenario

In the first scenario, it is assumed that the solar irradiation will produce $ISC = 5.61$ A in the PV module according to (21). The MPPT control block, shown in Fig. 7, determines the requested PV module voltage V^*_{dc} , which is 117.3 V to achieve the maximum power from the PV system that can generate 558 W of electrical power. The requested active power to be transmitted to the grid is initially set at 662W and is changed to 445W at time $t = 40$ ms and the reactive power changes from zero to 250 VAR at time $t = 100$ ms. Fig. 9 shows the results of the first scenario simulation. Fig. 9(a) and (b) shows that the proposed control system has correctly followed the requested active and reactive power, and Fig. 9(c) shows that the PV voltage has been controlled accurately (to be 177.3 V) to obtain the maximum power from the PV module. Fig. 9(d) shows that battery is discharging when the grid power is more than the PV power, and it is charging when the PV power is more than the grid power. Fig. 9(d) shows that before time $t = 40$ ms, the battery discharges at 1.8 A since the power generated by the PV is insufficient. After time $t = 40$ ms, the battery current is about

-1.8 A, signifying that the battery is being charged from the extra power of the PV module. Fig. 9(e) shows the inverter ac-side currents, and Fig. 9(f) shows the grid-side currents with a THD less than 1.29% due to the LCL filter. The simulation results in Fig. 9 show that the whole system produces a very good dynamic response. Fig. 10 shows the inverter waveforms for the same scenario. Fig. 10(a) shows the line-to-line voltage V_{ab} , and Fig. 10(b) shows the phase to midpoint voltage of the inverter V_{ao} . Fig. 10(c) and (e) shows V_{ao} , V_{on} , and V_{an} after mathematical filtering to determine the average value of the PWM waveforms.

Fig. 9. Simulated results for the first scenario. (a) Active power injected to the grid. (b) Reactive power injected to the grid. (c) PV module DC voltage. (d) Battery current. (e) Inverter AC current. (f) Grid current.

(a)
=
(b)

Fig 10 Total Harmonic Distortion of the Three Level NPC Output Current (a) Using PI Controller (b) Using Fractional Order PID

Figure 10 show that Fractional Order PID Controller can achieve the less THD Values (4.18%) when compared with Traditional PI Controller (i.e. 12.42%).

B. Second Theoretical Scenario

In the second scenario, it is assumed that the solar irradiation will change such that the PV module will produce $I_{SC} = 4.8, 4,$ and 5.61 A. The MPPT control block determines that V_{dc} needs to be 115.6, 114.1, and 117.3 V to achieve the maximum power from the PV units which can generate 485, 404, and 558 W, respectively. The requested active power to be transmitted to the grid is set at a constant 480 W and the reactive power is set to zero during the simulation time. Fig. 11 shows the results of the second scenario simulation. Fig. 11(a) shows that the inverter is able to generate the requested active power. Fig. 11(b) shows that the PV voltage was controlled accurately for different solar irradiation values to obtain the relevant maximum power from the PV modules. Fig. 11(c) shows that the charging and discharging of the battery are correctly performed. The battery has supplemented the PV power generation to meet the requested demand by the grid. Fig. 11(d) illustrates that the quality of the waveforms of the grid-side currents are acceptable, which signifies that the correct PWM vectors are generated by the proposed control strategy. By using the proposed strategy, the inverter is able to provide a fast transient response. Fig. 11(e) shows the a-phase voltage

Fig. 10. Simulated inverter waveforms. (a) V_{ab} -Phase to phase inverter voltage. (b) V_{ao} -Inverter phase voltage reference to midpoint. (c) Filtered V_{on} -Filtered inverter phase voltage reference to midpoint. (d) Filtered V_{on} -

Filtered midpoint voltage reference to neutral. (e) Filtered Van-Filtered phase voltage reference to neutral. and current of the grid, which are always in-phase signifying that the reactive power is zero at all times.

C. Practically Oriented Simulation

In the third simulation, the requested active power to be transmitted to the grid is initially set at 295 W and, at time $t = 40$ ms, the requested active power starts to reduce as a slope controlled change and is finally stays constant at 165 W at $t = 90$ ms. It is assumed that the solar irradiation will produce $I_{SC} = 2.89$ A in the PV module according to (21). The requested PV module voltage V_{dc} , to achieve MPPT condition will be 112.8 V to generate 305 W of electrical power. Fig. 12(a) shows that the active power transmitted to the grid reduces and follows the requested active power. Fig. 12(b) shows the battery current which is about 0.1 A before $t = 40$ ms and then because of the reduced power transmission to the grid with constant PV output, the battery charging current is increased and finally fixed at about 2.2 A. Fig. 12(c) shows the ac inverter currents slowly decreasing starting from 3.4 Arms at $t = 40$ ms and finally stays constant at 1.9 Arms at $t = 90$ ms. During this simulation, the dc voltage is held at 112.8 V to fulfill the MPPT requirement. It is important to note that during the simulations, the dc bus is working under unbalanced condition because the battery voltage during the simulation is equal to 60 V, and therefore, this particular scenario will not allow equal capacitor voltages.

Fig. 11. Simulated results for the second scenario. (a) Active power injected to the grid. (b) PV module DC voltage. (c) Battery currents. (d) Grid side currents. (e) Grid side Phase (a) voltage and its current.

VI. CONCLUSION

A Three phase voltage source inverter that can integrate both renewable energy and battery storage on the dc side of the inverter has been presented. A theoretical framework of a novel extended unbalance three-level vector modulation technique and Fractional Order PID Controller that can generate the correct ac voltage under unbalanced dc voltage conditions has been proposed. The effectiveness of the proposed topology and Fractional Order PID Controller was tested using MATLAB/SIMULINK and results are presented. The MATLAB results demonstrate that the proposed system is able to control ac-side current, and battery charging and discharging currents at different levels of solar irradiation. The Proposed Fractional Order PID control Strategy concludes that decreases 4.18% from 12.42% THD Values of Three Level NPC Output Current.

VII. ACKNOWLEDGMENT

I greatly Indebted for forever to my Guide, to my HOD K .Chandra Obula Reddy and all teaching and non-teaching staff who supported directly and indirectly to complete my work. I sincerely thankful to my principal Dr.

S.K. Biradar for continue encouragement and active interest in my progress throughout the work. I am grateful being a M.tech Electrical Power System student of Matsyodari Shikshan Sanstha's College of Engineering and Technology, Jalna, Maharashtra.

REFERENCES

- [1] O. M. Toledo, D. O. Filho, and A. S. A. C. Diniz, "Distributed photovoltaic generation and energy storage systems: A review," *Renewable Sustainable Energy Rev.*, vol. 14, no. 1, pp. 506–511, 2010.
- [2] M. Bragard, N. Soltau, S. Thomas, and R. W. De Doncker, "The balance of renewable sources and user demands in grids: Power electronics for modular battery energy storage systems," *IEEE Trans. Power Electron.*, vol. 25, no. 12, pp. 3049–3056, Dec. 2010.
- [3] A. Yazdani and P. P. Dash, "A control methodology and characterization of dynamics for a photovoltaic (PV) system interfaced with a distribution network," *IEEE Trans. Power Del.*, vol. 24, no. 3, pp. 1538–1551, Jul. 2009.
- [4] A. Yazdani, A. R. Di Fazio, H. Ghoddami, M. Russo, M. Kazerani, J. Jatskevich, K. Strunz, S. Leva, and J. A. Martinez, "Modeling guidelines and a benchmark for power system simulation studies of three-phase single-stage photovoltaic systems," *IEEE Trans. Power Del.*, vol. 26, no. 2, pp. 1247–1264, Apr. 2011.
- [5] M. A. Abdullah, A. H. M. Yatim, C. W. Tan, and R. Saidur, "A review of maximum power point tracking algorithms for wind energy systems," *Renewable Sustainable Energy Rev.*, vol. 16, no. 5, pp. 3220–3227, Jun. 2012.
- [6] S. Burusteta, J. Pou, S. Ceballos, I. Marino, and J. A. Alzola, "Capacitor voltage balance limits in a multilevel-converter-based energy storage system," in *Proc. 14th Eur. Conf. Power Electron. Appl.*, Aug./Sep. 2011, pp. 1–9.
- [7] L. Xinchun, Shan Gao, J. Li, H. Lei, and Y. Kang, "A new control strategy to balance neutral-point voltage in three-level NPC inverter," in *Proc. IEEE 8th Int. Conf. Power Electron. ECCE Asia*, May/Jun. 2011, pp. 2593–2597.
- [8] J. Rodriguez, S. Bernet, P. K. Steimer, and I. E. Lizama, "A survey on neutral-point-clamped inverters," *IEEE Trans. Ind. Electron.*, vol. 57, no. 7, pp. 2219–2230, Jul. 2010.
- [9] A. Lewicki, Z. Krzeminski, and H. Abu-Rub, "Space-vector pulsewidth modulation for three-level npc converter with the neutral point voltage control," *IEEE Trans. Ind. Electron.*, vol. 58, no. 11, pp. 5076–5086, Nov. 2011.
- [10] J. Pou, D. Boroyevich, and R. Pindado, "Effects of imbalances and nonlinear loads on the voltage balance of a neutral-point-clamped inverter," *IEEE Trans. Power Electron.*, vol. 20, no. 1, pp. 123–131, Jan. 2005.
- [11] Z. Huibin, S. Jon Finney, A. Massoud, and B. W. Williams, "An SVM algorithm to balance the capacitor voltages of the three-level npc active power filter," *IEEE Trans. Power Electron.*, vol. 23, no. 6, pp. 2694–2702, Nov. 2008.